Strojniški vestnik - Journal of Mechanical Engineering vol(yyyy)no, p-p
Received for review: yyyy-mm-dd

Received revised form: yyyy-mm-dd
DOI code
Original / Review / Short Scientific Paper
Accepted for publication: yyyy-mm-dd

# Determining Optimum Rotary Blade Design for Wind Power Water Pumping System for Local Selected Sites

Abdulbasit Mohammed[1], Hirpa G. Lemu[2,*], Belete Sirahbizu[1]
[1] Addis Ababa Science and Technology University, Ethiopia
[2] University of Stavanger, Norway

*The design of windmill rotor is essentially important to harness the wind energy. In this work a study is conducted to optimize the design and performance of rotor blade that is suitable for low wind condition. The windmills' rotor blades are aerodynamically designed based on SG6043 airfoil and wind speed data at local selected sites. The aerodynamic profile of the rotor blade that can provide a maximum power coefficient, which is the relation between real rotor performance and the available wind energy on a given reference areas was calculated. Different parameters such as blade shapes, chord distributions, tip speed ratio, geometries set angles, etc., were used to optimize the blade design with an objective of extracting maximum wind power for water pumping system and wind mill rotors size of 10.74 m, 7.34 m, and 6.34 m diameter with 3 blades were obtained for the selected sites at Abomsa, Metehara and Ziway in South-east Ethiopia. During the rotary blades performance optimization, Blade Element Momentum (BEM) theory and solving iteration by MATLAB® coding were used.*

**Keywords: Boundary element method, rotary sizing, wind power, hydraulic power, power coefficient, water pumping system**

**Highlights**:

- Optimum rotary blade for wind power at low wind speed has been designed based on SG603 airfoil and analysed for three selected local sites.
- The blade design is optimized with an objective of extracting maximum wind power for each selected site for the purpose of water pumping system.
- The relation between real rotor performance and the available wind energy on the selected given reference areas is calculated to find the optimum aerodynamic profile of the blades.
- Blade Element Momentum theory has been used and iterated in MATLAB to identify the parameters for the performance optimization.

## 0 INTRODUCTION

Nowadays, there exists significant global progress to benefit from the need of renewable energy by converting the energy in the wind to a mechanical form by designing and constructing diverse forms of windmills [1]. The main interest in energy from the wind is that the conversion process does not release carbon emission to environment, and it leads to less consumption of resources. In order to mitigate the side effects of fossil fuels, the use of renewable energy sources has become extremely important. In this respect, wind energy is considered to be one of the most promising renewable energy sources which can be continuously generated by force of nature, and the rotor blade design is decisive to be able to optimally harvest the wind energy.

Studies on wind turbine rotor blade design have been continuously conducted based on the performance of aerodynamic analysis. Supreeth et al. [2] used heuristic approach to study rotary blade design for a fixed pitch and small-scale horizontal axis wind turbine. The sectional chord and twist angle distribution for the idealized, optimized and linearized blades was analytically determined. Prasad et al. [3] designed the rotary blade of windmills for irrigational purposes at Bagur of Hosadurga district (Karnataka) site. Various parameters were optimized to achieve maximum power coefficient. Lopez-Lopez, et al. [4] studied the effect of the blade slenderness and the wind speed on the dynamics and instability of wind turbine blade under large deflection. They used a simple cantilever beam model and employed Galerkin approach, which is validated with

*Corr. Author's Address: University of Stavanger, N-4036, Stavanger, Norway, Hirpa.g.lemu@uis.no

experimental results. Sang et al. [5] have also improved an optimization framework for blade aerodynamic design under realistic conditions. The design parameters, such as angle of twist, chord distribution and maximum chord and the objective function relation were obtained. Shubham et al. [6] designed and optimized the micro wind turbine blades at rated wind speed of 8.4 m/s using QBlade, where SG6043 airfoil was selected and 1.2 m blade length Simulation was done. Zin [7] reported the design of 1.2 kW wind turbine blade for rural application for Mandalay Hill of Mandalay City in Myanmar at rated wind velocity of 7 m/s. The blade airfoil, angle of pitches and distribution of sectional chord along the blade span were determined. Deepak et al. [8] designed and optimized the blade of small wind turbine by considering the various factors such as tip loss, hub loss, drag coefficient, and wake. By using blade element momentum methods (BEM), power performance was simulated. Hani et al. [9] optimized the rotor blade parameters that have effect on blade design for small turbines having low performance due to low Reynolds number. In optimization processes, the performance of the final designed blade performance was investigated by employing the blade element momentum theory. Naveen et al. [10] designed 300 W micro horizontal axis wind turbine using BEM theory on SG6040 and SG6041 airfoils. The BEM procedure was codified in MATLAB software and a 3 m diameter wind turbine was analysed with QBlade. In general, the literature study indicates that the efficient conversion of the wind energy directly to a mechanical form requires closer study of the local wind data and designing rotor blades that are tailor made for the wind condition.

This study focused on designing optimum rotary blades for wind power water pumping system for local selected sites at Abomsa, Metehara and Ziway in Ethiopia. This design of the blades is based on design of aerodynamic type of SG6043 airfoil reported by Giguere and Selig [11, 12] (and analysis of collected wind speed data of the sites [13] from National Meteorological Agency (NMA). The blade parameters including chord distribution length, angle of wind relative wind, angle of twist, tip speed ratio, power coefficient of the blade, and attack angle were determined. These blades parameters were optimized to attain maximum power coefficients with using Blade Element Momentum (BEM) theory procedures and different iterations were solved by MATLAB coding.

## 1 DESIGN METHODS AND PROCEDURES

The general procedures followed to design the rotor blades of the windmills for water pumping application are summarized in Fig. 1.


**Fig. 1**: *Design procedure of rotary blade of wind turbines*

The weather data was collected from selected local cites: Abomsa, Metehara and Ziyay, all from Eastern part of the Oromia regional state, Ethiopia. The next step is developing new designs and configurations of the rotor blades (rotor blade sizing) that can efficiently transform the energy in the wind to a direct mechanical energy to drive water pumps. Figure 2 describes the design steps that must be taken to determine the optimum rotary size of windmills to be used at those particular sites and for a particular purpose.

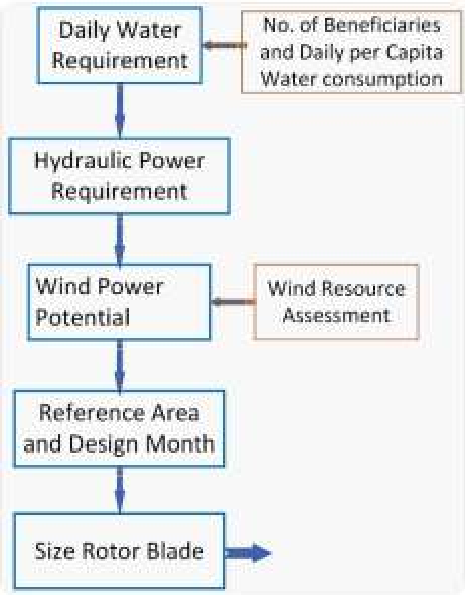


**Fig. 2**: *Illustration of the design steps for sizing of wind mill rotor for water pumping system.*

*Daily Water Requirement ($Q_D$):* This depends on the total number of beneficiaries ($N_B$) of the site and the daily water consumptions per capita ($q_{pp}$), expressed as Eq.1.

$$Q_D = N_B * q_{pp} \quad (1)$$

*Hydraulic power requirement* ($P_{Hyd}$)***:*** This parameter is a function of the daily water requirement *($Q_D$)* and total pumping head (*H*) as given by Eq. 2 [14, 16], where the total pumping head includes the static water head *($H_{St}$)* and friction losses *($H_{fr}$),* considering losses on the pipe, minor losses and velocity head.

$$P_{hyd} = 0.113452 * Q_D * H \quad (2)$$

*where* $H = H_{St} + H_{fr}$

*Wind Power Potential* ($P_{wind}$)*:* The availability of wind power potential on a monthly basis is very necessary to evaluate as given in Eq. 3. [14 - 18].

$$P_{Wind} = \frac{1}{2}\rho_{air} * V^3 \quad (3)$$

***Reference Area ($A_r$):*** Reference area is related to the rotor area needed to capture sufficient power from the wind as given in Eq. 4 [14-18].

$$A_r = \frac{P_{hyd}}{P_{wind}} \quad (4)$$

### 1.1 Blade design procedures

After rotary blade size of horizontal axis windmills was determined, the following steps were considered in rotary blade design.

**a.** *Determining the minimum $C_d$ / $C_l$ Ratio:* This is important to find out the value of design lift and angle of attack corresponding to a minimum value of $C_d/C_l$ ratio.

*b. Determining Design Lift coefficient and* design *angle of attack ($\alpha_d$)*: From airfoil data corresponding to minimum $C_d/C_l$ ratio, the value of lift coefficient and angle of attack are found.

*c. Choosing design Tip Speed Ratio (λ) and number of blades (B):* These parameters can be chosen from TSR vs. number of blade table depending on the form of operation.

*d. Determining geometries of optimum blades:* when rotor blade size is determined, then it is divided into 10-20 equal segments or elements, where for each unit element, the blade geometries such as local tip speed ratio $\lambda$ ($r_i$), relative wind angle $\psi$ ($r_i$), chord distribution *c ($r_i$),* pitch angle $\theta$ ($r_i$), twist angle $\phi$ ($r_i$), and local solidity $\sigma$ ($r_i$), can be computed as shown in Fig. 3.

e. *Linearization of the twist angle and blade chord length:* Using the optimum blade shapes as a guide, a blade shape that promises to be a good approximation is selected. Since the chords as well as the blade twist vary in a non-linear manner along the blade, it is possible to linearize the chords and the twist angles using Eq. 5.

$$c(r_i) = a_1 r_i + a_2 \qquad (5)$$
$$\phi(r_i) = a_3(R - r_i)$$

Where $a_1$, $a_2$ and $a_3$ are constant coefficients obtained from the chosen chord distributions and twist angles.

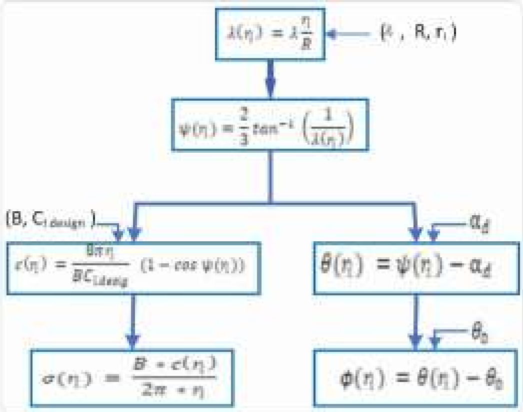


**Fig. 3***: Computation procedures to determine blade geometries*

### 1.2 Rotor blade performance

After chords and twist angles are linearized, the geometry of rotary blade gets practical shape. The performance of designed rotor blade is conducted by using BEM theory [19]. Obtaining axial $a$ $(r_i)_j$, and angular induction factors $\acute{a}(r_i)_j$ of the designed blade is the base of rotor blade performances. It is possible to determine the inflow angle using the axial and angular induction factors as follows (Eq. 6).

$$\psi(r_i) = tan^{-1}\left(\frac{1 - a(r_i)_j}{\left(1 + \acute{a}(r_i)_j\right)}\frac{1}{\lambda(r_i)}\right) \quad (6)$$

To describe the lifting power reduction by airflow around the blade tip, the tip loss correction factor *F($r_i$)* for each *i*th section is calculated based on Prandtl's method [20]:

$$F(r_i) = \left(\frac{2}{\pi}\right) cos^{-1}\left[e^{-\left(\frac{\frac{B}{2}\left(1-\frac{r_i}{R}\right)}{\frac{r_i}{R} sin\,\psi(r_i)}\right)}\right] \quad (7)$$

The axial and tangential induction factors for each sectional $i^{th}$ element at iteration $j^{th}$ are then calculated using Eq. 8. If the axial induction factor is greater than 0.4, the Froude momentum principle is no longer accurate. Thus, Galih [21] suggested correction of the axial induction factor, if $a(r_i)_j$ > $a_c$, using Eq. 9.

$$a(r_i)_j = \left(\frac{4\,F(r_i)\sin^2\psi(r_i)}{\sigma_{r,i}(C_{l,i}\,cos\,\psi(r_i) + C_{d,i}\,sin\,\psi(r_i))} + 1\right)^{-1}$$
$$\acute{a}(r_i)_j = \left(\frac{4\,F(r_i)\cos\psi(r_i)\sin\psi(r_i)}{\sigma(r_i)(C_{l,i}\,sin\,\psi(r_i) - C_{d,i}\,cos\,\psi(r_i))} - 1\right)^{-1} \quad (8)$$

$$a(r_i)_j = \frac{1}{2}\left\{2 + Z(r_i) - \sqrt{(Z(r_i)(1-2a_c)+2)^2 + 4(Z(r_i)a^2{}_c - 1)}\right\} \quad (9)$$

Where $a_c$ is commonly about 0.2 and $Z(r_i)$ is defined as:

$$Z(r_i) = \frac{4\,F(r_i)\sin^2\psi(r_i)}{\sigma(r_i)(C_{l,i}\,cos\,\psi(r_i) + C_{d,i}\,sin\,\psi(r_i))} \quad (10)$$

Finally, the local thrust $C_T(r_i)$ and power coefficient $C_P(r_i)$ can be computed from the following relations.

$$C_T(r_i) = \sigma(r_i)\left(1 - a(r_i)_j\right)^2 \frac{(C_{l,i}\,cos\,\psi(r_i) + C_{d,i}\,sin\,\psi(r_i))}{F(r_i)\,sin^2\,\psi(r_i)} \quad (11)$$

$$C_P(r_i) = \frac{8}{\lambda^2}F(r_i)\,\lambda^3(r_i)\,\acute{a}(r_i)_j \left(1 - a(r_i)_j\right)\left(1 - \frac{C_d}{C_l}\right)\cot\psi(r_i)$$

## 2 ANALYSIS OF RESULTS

The rotary blades have been designed according to data collected National Meteorological Agency (NMA) of Ethiopia from three selected sites (Abomsa, Metehara and Ziway). The data was collected for 1-year (October 2018 to September 2019) period at 10 m height. and Table 1 shows important data determined from the three selected sites and total water demand and pumping required can be calculated by estimating the daily water consumption per capita to be 20 L/person in Ethiopia [14, 15]. The monthly mean wind speeds were extrapolated at 20 m heights (hub heights) and monthly specific wind power potential for the three selected sites were evaluated (Table 2).

**Table 1**: *Important parameters for three selected sites*

| Parameters | Abomsa | Metehara | Ziway |
|---|---|---|---|
| No of beneficiary | 4086 | 4191 | 3867 |
| Total demand (L) | 81720 | 83820 | 77340 |
| Pumping required ($m^3$/day) | 81.72 | 83.82 | 77.34 |
| Total Head (m) | 87 | 79 | 74 |
| Tip speed ratio (λ) | 3 | 3.5 | 4 |
| Number of blade (B) | 3 | 3 | 3 |

Based on the number of beneficiaries and total water demands, hydraulic power can be determined which is constant through the year, reference area and rotor diameter for the three sites were calculated and summarized in Table 3. The rotor size is chosen on the basis of "design month", which is the month in which the water demand is highest in relation to the wind power resources, i.e. the month when the system will be most heavily loaded [14], [16]. Therefore, according to the data given in Table 3, August, March and April are design months for Abomsa, Metehara and Ziway respectively.

For three rotor blade design, Selig and Gigueŕe recommended airfoil type SG6043 [11, 12] for low Reynolds numbers because this type airfoils operate in regional low wind speed. The designed $C_l$ and $C_l/C_d$ graphs characteristics of SG6043 with Re of $0.23*10^6$, $0.25*10^6$ and $0.29*10^6$ are evaluated, as illustrated in Fig. 4, using QBlade, for Abomsa, Metehara and Ziway respectively. Fig. 5 shows that the general flow diagram for determining blade geometries and performing the designed blades by iterating axial and tangential induction factors.

**Table 2**: *Available mean wind speeds and specific wind power for three selected sites*

| Year | Month | Abomsa | | | Metehara | | | Ziway | | |
|---|---|---|---|---|---|---|---|---|---|---|
| | | $V_m$@10 (m/s) | $V_m$@20 (m/s) | $P_{wind}$ (w) | $V_m$@10 (m/s) | $V_m$@20 (m/s) | $P_{wind}$ (w) | $V_m$@10 (m/s) | $V_m$@20 (m/s) | $P_{wind}$ (w) |
| 2018 | Oct | 2.82 | 3.42 | 24.59 | 2.93 | 3.56 | 27.58 | 3.82 | 4.64 | 61.12 |
| | Nov | 2.81 | 3.41 | 24.33 | 2.72 | 3.30 | 22.06 | 3.92 | 4.76 | 66.04 |
| | Dec | 2.99 | 3.63 | 29.31 | 2.63 | 3.19 | 19.95 | 3.56 | 4.32 | 49.47 |
| 2019 | Jan | 3.82 | 4.64 | 61.12 | 2.63 | 3.19 | 19.95 | 3.67 | 4.46 | 54.20 |
| | Feb | 3.63 | 4.41 | 52.44 | 2.92 | 3.55 | 27.30 | 3.05 | 3.70 | 31.11 |
| | Mar | 3.27 | 3.97 | 38.34 | 2.53 | 3.07 | 17.76 | 2.91 | 3.53 | 27.02 |
| | Apr | 2.33 | 2.83 | 13.87 | 2.65 | 3.22 | 20.40 | 2.66 | 3.23 | 20.64 |
| | May | 2.76 | 3.35 | 23.05 | 2.75 | 3.34 | 22.80 | 3.01 | 3.65 | 29.90 |
| | Jun | 2.58 | 3.13 | 18.83 | 3.39 | 4.12 | 42.71 | 4.14 | 5.03 | 77.80 |
| | July | 2.42 | 2.94 | 15.54 | 3.36 | 4.08 | 41.59 | 3.20 | 3.89 | 35.93 |
| | Aug | 2.01 | 2.44 | 8.90 | 3.23 | 3.92 | 36.95 | 3.64 | 4.42 | 52.88 |
| | Sept | 2.16 | 2.62 | 11.05 | 2.75 | 3.34 | 22.80 | 2.72 | 3.30 | 22.06 |

**Table 3**: *Hydraulic power, reference area and rotor diameter for three selected sites*

| Year | Month | Abomsa | | | Metehara | | | Ziway | | |
|---|---|---|---|---|---|---|---|---|---|---|
| | | $P_{hyd}$ | $A_r$ | $D_r$ | $P_{hyd}$ | $A_r$ | $D_r$ | $P_{hyd}$ | $A_r$ | $D_r$ |
| 2018 | Oct | 806.3 | 32.8 | 6.5 | 750.9 | 27.2 | 5.9 | 649.1 | 10.6 | 3.7 |
| | Nov | 806.3 | 33.1 | 6.5 | 750.9 | 34.0 | 6.6 | 649.1 | 9.8 | 3.5 |
| | Dec | 806.3 | 27.5 | 5.9 | 750.9 | 37.7 | 6.9 | 649.1 | 13.1 | 4.1 |
| 2019 | Jan | 806.3 | 13.2 | 4.1 | 750.9 | 37.7 | 6.9 | 649.1 | 12.0 | 3.9 |
| | Feb | 806.3 | 15.4 | 4.4 | 750.9 | 27.5 | 5.9 | 649.1 | 20.9 | 5.2 |
| | Mar | 806.3 | 21.0 | 5.2 | 750.9 | 42.3 | 7.3 | 649.1 | 24.0 | 5.5 |
| | Apr | 806.3 | 58.1 | 8.6 | 750.9 | 36.8 | 6.9 | 649.1 | 31.5 | 6.3 |
| | May | 806.3 | 35.0 | 6.7 | 750.9 | 32.9 | 6.5 | 649.1 | 21.7 | 5.3 |
| | Jun | 806.3 | 42.8 | 7.4 | 750.9 | 17.6 | 4.7 | 649.1 | 8.3 | 3.3 |
| | July | 806.3 | 51.9 | 8.1 | 750.9 | 18.1 | 4.8 | 649.1 | 18.1 | 4.8 |
| | Aug | 806.3 | 90.6 | 10.7 | 750.9 | 20.3 | 5.1 | 649.1 | 12.3 | 4.0 |
| | Sept | 806.3 | 73.0 | 9.6 | 750.9 | 32.9 | 6.5 | 649.1 | 29.4 | 6.1 |

The blade geometries are determined with number of segments or elements (N) equal to 15. The local chord distributions, geometries set angles and solidities of optimal and linearized blades for three selected sites are determined and summarized in Table 4, 5 and 6. The comparison of blade chord distributions and sectional angles of twist for optimal and linearized blades for three selected sites are illustrated in Fig. 6.

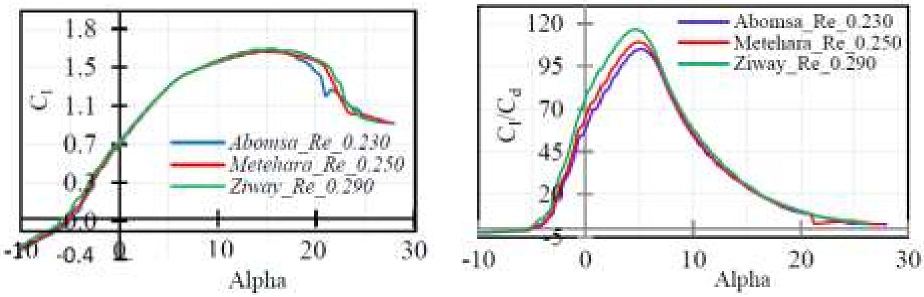


**Fig. 4** *Lift Coefficient $C_l$ and $C_l/C_d$ of SG6043 with Reynolds numbers of three sites.*

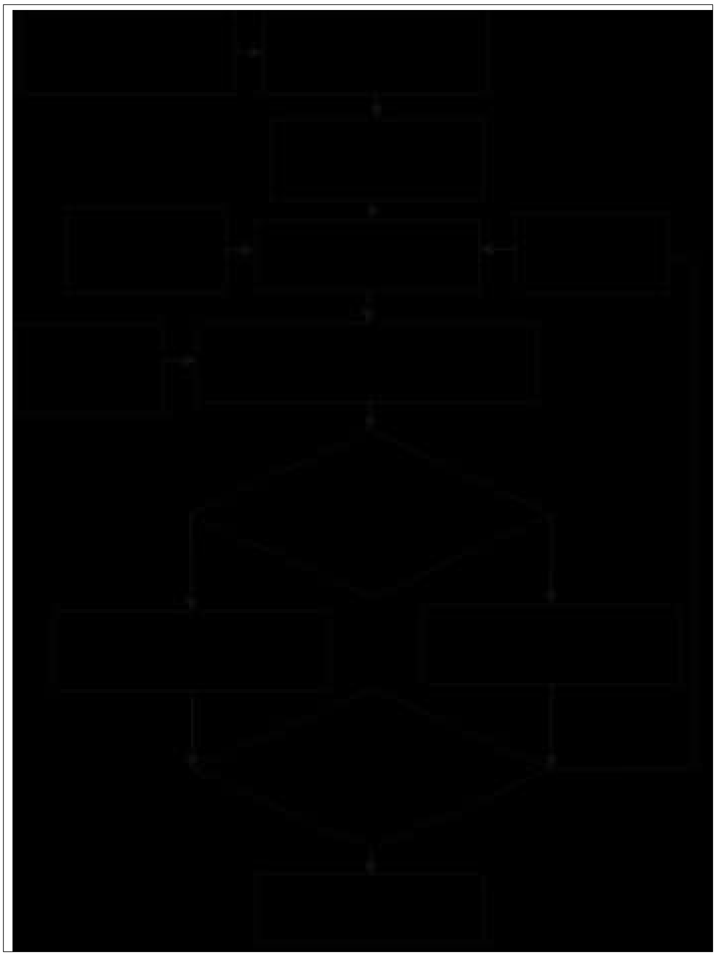

**Fig. 5**: *Flow diagram of performing rotor blades design*

**Table 4**: *Geometrical properties of optimum and linearized rotor blades for Abomsa site*

| | Optimal Blade | | | | Linearized Blade | | | |
|---|---|---|---|---|---|---|---|---|
| $r_i/R$ | $\psi(r_i$ | $\theta(r_i),$ | $\phi(r_i)$ | $c(r_i)$ | $\psi(r_i$ | $\theta(r_i)$ | $\phi(r_i)$ | $c(r_i)$ |
| 0.07 | 52.46 | 47.46 | 40.17 | 0.39 | 24.83 | 19.83 | 20.79 | 0.77 |
| 0.13 | 45.47 | 40.47 | 33.18 | 0.59 | 23.34 | 18.34 | 19.30 | 0.73 |
| 0.20 | 39.36 | 34.36 | 27.07 | 0.68 | 21.86 | 16.86 | 17.82 | 0.70 |
| 0.27 | 34.23 | 29.23 | 21.94 | 0.69 | 20.37 | 15.37 | 16.33 | 0.67 |
| 0.33 | 30.00 | 25.00 | 17.71 | 0.66 | 18.89 | 13.89 | 14.85 | 0.64 |
| 0.40 | 26.54 | 21.54 | 14.25 | 0.63 | 17.40 | 12.40 | 13.36 | 0.61 |
| 0.47 | 23.69 | 18.69 | 11.40 | 0.59 | 15.92 | 10.92 | 11.88 | 0.58 |
| 0.53 | 21.34 | 16.34 | 9.05 | 0.54 | 14.43 | 9.43 | 10.39 | 0.54 |
| 0.60 | 19.37 | 14.37 | 7.08 | 0.51 | 12.95 | 7.95 | 8.91 | 0.51 |
| 0.67 | 17.71 | 12.71 | 5.42 | 0.47 | 11.46 | 6.46 | 7.42 | 0.48 |
| 0.73 | 16.30 | 11.30 | 4.01 | 0.44 | 9.98 | 4.98 | 5.94 | 0.45 |
| 0.80 | 15.08 | 10.08 | 2.79 | 0.41 | 8.49 | 3.49 | 4.45 | 0.42 |
| 0.87 | 14.03 | 9.03 | 1.74 | 0.38 | 7.01 | 2.01 | 2.97 | 0.39 |
| 0.93 | 13.10 | 8.10 | 0.81 | 0.36 | 5.52 | 0.52 | 1.48 | 0.35 |
| 1.00 | 12.29 | 7.29 | 0.00 | 0.34 | 4.04 | -0.96 | 0.00 | 0.32 |

**Table 5**: *Geometrical properties of optimum and linearized rotor blade for Metehara site*

| | Optimal Blade | | | | Linearized Blade | | | |
|---|---|---|---|---|---|---|---|---|
| $r_i/R$ | $\psi(r_i$ | $\theta(r_i)$, | $\phi(r_i)$ | $c(r_i)$ | $\psi(r_i$ | $\theta(r_i)$ | $\phi(r_i)$ | $c(r_i)$ |
| 0.07 | 51.24 | 46.24 | 40.61 | 0.43 | 23.04 | 18.04 | 18.98 | 0.73 |
| 0.13 | 43.32 | 38.32 | 32.69 | 0.63 | 21.68 | 16.68 | 17.62 | 0.70 |
| 0.20 | 36.67 | 31.67 | 26.04 | 0.69 | 20.33 | 15.33 | 16.27 | 0.66 |
| 0.27 | 31.32 | 26.32 | 20.69 | 0.67 | 18.97 | 13.97 | 14.91 | 0.63 |
| 0.33 | 27.07 | 22.07 | 16.44 | 0.63 | 17.62 | 12.62 | 13.56 | 0.60 |
| 0.40 | 23.69 | 18.69 | 13.06 | 0.59 | 16.26 | 11.26 | 12.20 | 0.57 |
| 0.47 | 20.98 | 15.98 | 10.35 | 0.54 | 14.91 | 9.91 | 10.85 | 0.54 |
| 0.53 | 18.79 | 13.79 | 8.16 | 0.49 | 13.55 | 8.55 | 9.49 | 0.50 |
| 0.60 | 16.98 | 11.98 | 6.35 | 0.45 | 12.19 | 7.19 | 8.13 | 0.47 |
| 0.67 | 15.47 | 10.47 | 4.84 | 0.42 | 10.84 | 5.84 | 6.78 | 0.44 |
| 0.73 | 14.19 | 9.19 | 3.56 | 0.39 | 9.48 | 4.48 | 5.42 | 0.41 |
| 0.80 | 13.10 | 8.10 | 2.47 | 0.36 | 8.13 | 3.13 | 4.07 | 0.38 |
| 0.87 | 12.16 | 7.16 | 1.53 | 0.34 | 6.77 | 1.77 | 2.71 | 0.35 |
| 0.93 | 11.35 | 6.35 | 0.72 | 0.32 | 5.42 | 0.42 | 1.36 | 0.31 |
| 1.00 | 10.63 | 5.63 | 0.00 | 0.30 | 4.06 | -0.94 | 0.00 | 0.28 |

**Table 6:** *Geometrical properties of Optimum and linearized rotor blades for Ziway site*

| | Optimal Blade | | | | Linearized Blade | | | |
|---|---|---|---|---|---|---|---|---|
| $r_i/R$ | $\psi(r_i$ | $\theta(r_i)$, | $\phi(r_i)$ | $c(r_i)$ | $\psi(r_i$ | $\theta(r_i)$ | $\phi(r_i)$ | $c(r_i)$ |
| 0.07 | 50.05 | 45.05 | 40.69 | 0.47 | 21.41 | 16.41 | 17.29 | 0.67 |
| 0.13 | 41.29 | 36.29 | 31.93 | 0.66 | 20.17 | 15.17 | 16.05 | 0.64 |
| 0.20 | 34.23 | 29.23 | 24.87 | 0.69 | 18.94 | 13.94 | 14.82 | 0.61 |
| 0.27 | 28.77 | 23.77 | 19.41 | 0.65 | 17.70 | 12.70 | 13.58 | 0.58 |
| 0.33 | 24.58 | 19.58 | 15.22 | 0.60 | 16.47 | 11.47 | 12.35 | 0.55 |
| 0.40 | 21.34 | 16.34 | 11.98 | 0.54 | 15.23 | 10.23 | 11.11 | 0.52 |
| 0.47 | 18.79 | 13.79 | 9.43 | 0.49 | 14.00 | 9.00 | 9.88 | 0.49 |
| 0.53 | 16.74 | 11.74 | 7.38 | 0.45 | 12.76 | 7.76 | 8.64 | 0.46 |
| 0.60 | 15.08 | 10.08 | 5.72 | 0.41 | 11.53 | 6.53 | 7.41 | 0.43 |
| 0.67 | 13.70 | 8.70 | 4.34 | 0.38 | 10.30 | 5.30 | 6.18 | 0.39 |
| 0.73 | 12.55 | 7.55 | 3.19 | 0.35 | 9.06 | 4.06 | 4.94 | 0.36 |
| 0.80 | 11.57 | 6.57 | 2.21 | 0.32 | 7.83 | 2.83 | 3.71 | 0.33 |
| 0.87 | 10.73 | 5.73 | 1.37 | 0.30 | 6.59 | 1.59 | 2.47 | 0.30 |
| 0.93 | 10.00 | 5.00 | 0.64 | 0.28 | 5.36 | 0.36 | 1.24 | 0.27 |
| 1.00 | 9.36 | 4.36 | 0.00 | 0.26 | 4.12 | -0.88 | 0.00 | 0.24 |

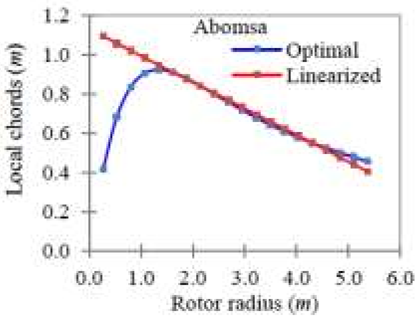


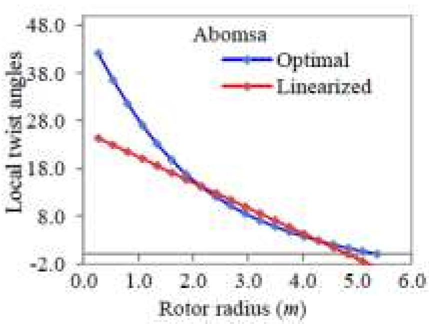

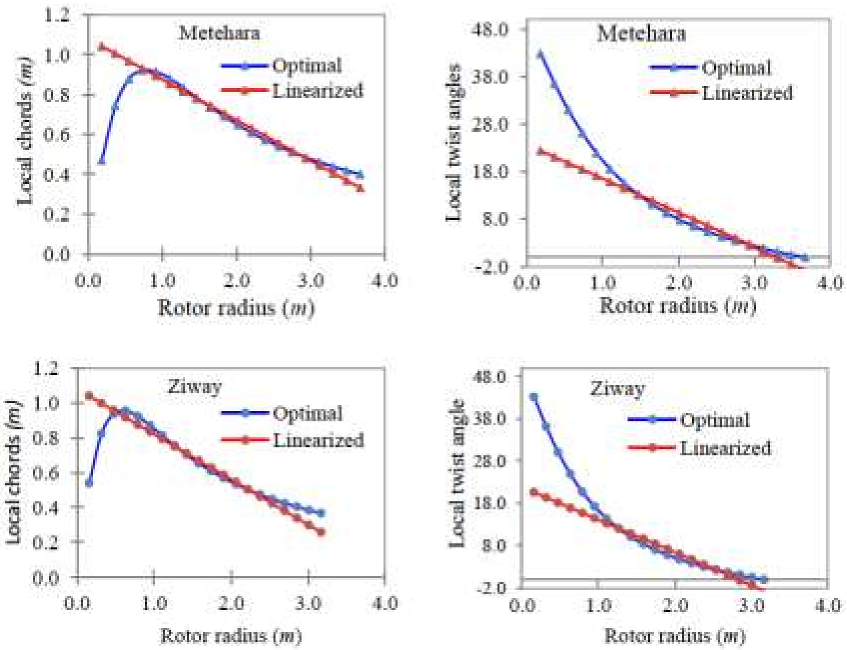


**Fig. 6**: *Local chord and twist angle comparison of optimal and linearized blades for three sites*

Base on the BEM flow diagram of iteration in Fig. 5, each local axial and tangential induction factors are converged after many iterations by MATALB coding and the coefficients of performance are illustrated as shown in Fig. 7 for these three local sites. The geometry profiles (shape) of designed and optimized rotor blades are modelled by QBlade software and the resulting blades are shown in Fig. 8. As can be observed from this figure, the maximum coefficient of performance values of $C_P\,(r_i)$ are 0.448, 0.459 and 0.463 at the maximum tip speed ratio of $\lambda(r_i)$ 3.0, 3.5 and 4.0 for the three sites Abomsa, Metehara and Ziway respectively. The geometry shape of optimal, linearized and optimized designed blades modelled by QBlade software and the resulting blades are shown in Fig. 8.

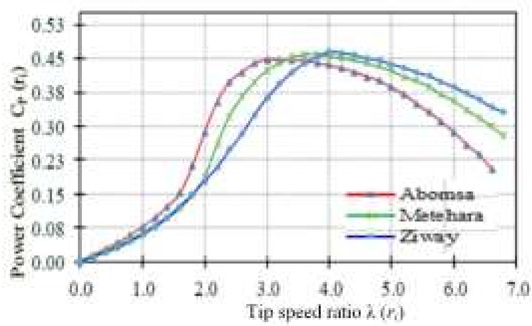


***Fig. 7***: *The $C_P(r_i)$ vs. $\lambda(r_i)$ of rotor performed blades for three selected sites.*

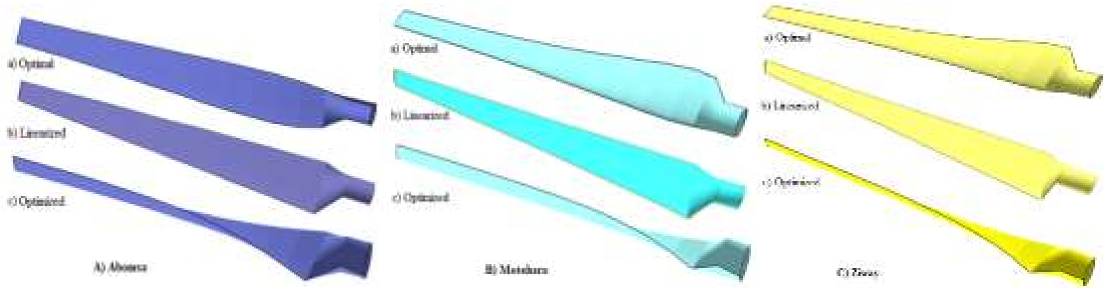

***Fig. 8***: *Geometry shape of optimal, linearized and optimized blades modelled by QBlade for A) Abomsa, B) Metehara and C) Ziway sites.*

## 3. CONCLUSION

In this study, the optimum rotary blade for wind power water pumping system for local three selected sites have been designed and analysed. From these designs, optimal blade parameters are determined, linearized and optimized. The geometry profiles of optimized blades are modelled by QBlade software for the three local selected sites. The key results of the design and analysis work show that the maximum coefficient of performance values $C_p(r_i)$ are 0.4512, 0.4587 and 0.4627 at the maximum tip speed ratio $\lambda(r_i)$ values of 3.0, 3.5 and 4.0 for the three sites Abomsa, Metehara and Ziway respectively. Furthermore, the average wind speeds at height of 20 m are 3.50 m/s, 3.60 m/s and 4.60 m/s respectively.

This article is part of a PhD research whose further work will focus on developing the design model of the blade with the obtained design specification and building a prototype wind turbine to test at the three locations.

## 4 NOMENCLATURE

### 4.1 Abbreviations

| | |
|---|---|
| $a(r_i)$: | Axial Induction Factors |
| $a'(r_i)$: | Angular Induction Factors |
| $a_1, a_2, a_3$: | Constant Coefficients |
| $A_r$: | Reference Area |
| $c(r_i)$: | Chord Distribution |
| $C_{d,i}$: | Local Drag Coefficient |
| $C_d$: | Drag Coefficient |
| $C_{l,i}$: | Local Lift Coefficient |
| $C_l$: | Lift Coefficient |
| $C_P(r_i)$: | Local Power Coefficient |
| $C_T(r_i)$: | Local Thrust Coefficient |
| $F(r_i)$: | Blade Tip Loss Factor |
| $H$: | Total Pumping Head |
| $H_{fr}$: | Friction Losses |
| $H_{st}$: | Static Water Head |
| $N_B$: | Total Number of Beneficiaries |
| $P_{hyd}$: | Hydraulic Power Requirement |
| $P_{wind}$: | Wind Power Potential |
| $Q_D$: | Daily Water Requirement |
| $q_{pp}$ | Water Consumption per Capita |
| $R$: | Rotor Blade Radius |
| $r_i$: | Local Radius |
| $V_m$: | Wind Velocity |

### 4.2 Symbols

| | |
|---|---|
| $\alpha_d$: | Design Attack Angle |
| $\theta(r_i)$: | Pitch Angle |
| $\lambda(r_i)$: | Local Tip Speed Ratio |
| $\lambda$: | Local Tip Speed Ratio |
| $\rho_{air}$: | Air Density |
| $\sigma(r_i)$: | Local Solidity |
| $\phi(r_i)$: | Twist Angle |
| $\psi(r_i)$: | Relative Wind Angle |

## 5 REFERENCES


[1]. Zuhair, E. A., Gowtham, R. (2015). Aero-design analysis for modified Darrieus based-straight bladed VAWT systems. *International Journal of Recent Technology and Engineering.* vol 4, no 5, pp 2321-7308.

[2]. Supreeth, R., Arokkiaswamy, A, Nagarjun, J.R., Prajwal, H.P, Sudhanva, M. (2019). Geometrical design of a rotor blade for a small-scale horizontal axis wind turbine. *International Journal of Recent Technology and Engineering*. vol 8, no 3, pp 2277-3878.

[3]. Prasad, S.S., Virupaxi A. (2012). Optimized design of rotor blade for a wind pump. *International Journal of Renewable Energy Research.* vol 2, no 4, (2012).

[4]. Lopez-Lopez, A., Robles-Ocampo, J.B., Sevilla-Camacho, P.Y., Lastres-Danguillecourt, O. Muniz, J., Perez-Sariñana, B.Y., de la Cruz, S. (2020). Dynamic instability of a wind turbine blade due to large deflections: An experimental validation, *SV – Journal of Mechanical Engineering*. vol 66, no 9, pp 523 – 533. DOI:10.5545/sv-jme.2020.6678.

[5]. Sang, L.L., SangJoon, S. (2020). Wind turbine blade optimal design considering multi-parameters and response surface method. *Energies.* vol 13, Doi: 10.3390/en13071639.

[6]. Shubham, R., Shubham, S., Rohan, S., Navjyot, S., Chaudhary, K. (2017). Simulation of micro wind turbine blade in QBlade. *International Journal for Research in Applied Science and Engineering Technology*. vol 5 (IV), pp 2321-9653.

[7]. Zin, M.C. (2019). Design calculation of 1200 W horizontal axis wind turbine blade for rural applications. *International Journal of Trend in Scientific Research and Development.* vol 3, no 5, pp 2456 – 6470.

[8]. Deepak, J., Chandan, R., Doddanna, K. (2017). Design & structural analysis of a small wind turbine blade for operation at low wind speed. *International Research Journal of Engineering and Technology*. vol 04, no 11, pp 2395-0072.

[9]. Hani, M., Wael, A., Waqar, K. (2020). Small wind turbine blade design and optimization. *Symmetry*. vol 12, no 18, Doi: 10.3390/sym12010018.

[10]. Naveen, P.N., Krishna, M. (2020). Design and analysis of micro horizontal axis wind turbine using MATLAB and QBlade. *International Journal of Advanced Science and Technology*. vol 9, no 10S, pp 8877-8885.

[11]. Gigueŕe, P. M. S., Selig, M.S. (1998). New airfoils for small horizontal, axis wind turbines. *Journal of Solar Energy Engineering*. vol. 120, no. 2, pp. 108–114.

[12]. Emmanuel, Y.O., Richard, O., Albert, K. S., Muyiwa S. A.: (2020). Development of high performance airfoils for application in small wind turbine power generation. *Journal of Energy*. vol 2020. Doi.org/10.1155/2020/9710189.

[13]. Mohammed, A., Lemu, H.G. Sirahbizu, B. (2020). Statistical analysis of Ethiopian wind power potential at selected sites, In: Proceedings of 8th EAI International Conference on Advancements of Science and Technology, Oct. 2 – 4, 2020, Bahir Dar, Ethiopia.

[14]. Ronak, D.G., Pramod, K., Debarshi, S., Bhushan, K., Shubham, C. (2015). Design and development of windmill operated water pump. *International Journal of Innovative Research in Science, Engineering and Technology.* vol 5, no. 1, pp 392 - 412.

[15]. Misrak, G., Marta, M., Abebayehu, A. (2015). Feasibility study of a wind powered water pumping system for rural Ethiopia. *AIMS Energy. vol* 3, no. 4, pp 851–868.

[16]. The Director A.W.F.: Ethiopia-Utilization of solar and wind energy for rural water supply in Ethiopia. Appraisal report, African Water Facility (2008).

[17]. Sathyajith, M. (2006). Wind energy fundamentals, resource analysis and economics. Springer Verlag Berlin Heidelberg, Library of congress control number: 2005937064 (2006).

[18]. Sultan, A. (2002). Investigation and analysis of wind pumping system for irrigation in Bangladesh. Bangladesh University of Engineering and Technology, PhD Thesis, Dhaka.

[19]. Kyoungboo, Y. (2020). Geometry design optimization of a wind turbine blade considering effects on aerodynamic performance by linearization. *Energies*, vol. 13, Doi: 10.3390/en13092320 (2020).

[20]. Burton, T., Sharpe, D. (2006). Wind energy handbook. John Wiley & Sons Ltd, Chichester.

[21]. Galih, B. (2018). Comparison of blade element method and CFD simulations of a 10 MW Wind Turbine. *Fluids*, vol. 3, no. 73. doi:10.3390/fluids3040073